Flexible glassy grid structure for rapid degradation of azo dye

R. Li[a,b], X. J. Liu[a]*, H. Wang[a], Y. Wu[a], K. C. Chan[b]*, Z. P. Lu[a]*

[a]State Key Laboratory for Advanced Metals and Materials, University of Science and

Technology Beijing, Beijing 100083, P. R. China

[b]Advanced Manufacturing Technology Research Centre, Department of Industrial and

Systems Engineering, The Hong Kong Polytechnic University, Hong Kong

Degradation of organic contaminants in industrial wastewaters has become a worldwide conundrum and attracted extensive attention. In this paper, we report a flexible grid structure with uniform mesh fabricated by plain weaving of melt spun $Fe_{80}B_{20}$ metallic glass micro-wires and the produced wire grid with a dosage of 0.3 g/L can almost completely degrade 0.2 g/L DB 15 azo dyes for less than 30 min at room temperature. The calculated degradation efficiency of the sample is approximately 4.3 min, 2.1 times faster than that of the $Fe_{80}B_{20}$ glassy ribbons and 28 times for commercial pure Fe powders. The enhanced degradation performance is primarily attributed to the uniform grid structure with high internal surface area in addition to the intrinsic activity of metallic glasses. Our findings not only provide high-performance candidate for degrading and filtering printing and dyeing wastewater with organic pollutant simultaneously, but also promote the broader applications of metallic glasses as functional materials.

*Corresponding author. E-mail: xjliu@ustb.edu.cn, kc.chan@polyu.edu.hk or luzp@ustb.edu.cn

1. Introduction

Due to the increasing demand of colorants and dyes in modern textile or other manufacturing industries, effective treatment of the organic wastewater has been becoming a worldwide conundrum [1-3]. Consequently, finding new approaches and developing of high-efficiency catalysts for the degradation of organic contaminants have become a research focus. In recent years, various degradation approaches and catalysts have been reported, such as flocculation by catalysts, adsorption onto active materials and catalytic or photocatalytic degradation by nanostructured materials [4-10]. Current economical approaches to degrading or decolorizing the organic wastewater contaminants generally include the reduction reaction or Fenton oxidation process by zero-valence metals, especially zero valent iron powders, which have attracted increasing industrial interests due to their low cost, efficient degradation activity and nontoxicity [11-16]. However, the high corrosion rate of crystalline elemental iron during degradation tend to result in rapid decay of the degradation efficiency [17, 18]. Meanwhile, agglomeration and difficult reclaim of pure micro/nano-scale Fe powders are also the handicap for their industrial applications. Consequently, developing novel materials with superior degradation efficiency have become a focus area in the field of dyeing wastewater treatment.

Metallic glasses (MGs), a novel class of metastable materials, have exhibited promising properties for catalytic applications due to their amorphous structure bearing no long-range order but abundant low-coordination sites at the surface [19-22]. Superior catalytic capability have been reported in degradation of azo dyes or removing

of organic matters in wastewater using some MGs as catalysts, such as Fe-, Mg-, MgZn-, and Co-based MGs [23-27]. Currently, most researches on MG catalysts are either based on the form of ribbons or powders. However, for glassy ribbons, their low specific surface area limits the degradation efficiency, while for glassy micro/nano-scale powders, the potential problems as reported in crystalline powders (e.g., agglomeration, clogging and recycling) still remain to be solved. To further enhance degradation performance, lifetime and recyclability of MG catalysts, design of new material forms is needed.

In this paper, a wire-woven grid structure of Fe-based MGs with excellent performance in degrading organic chemicals is newly designed and reported. Fabrication strategy of the glassy wire grid involves the melt spinning method to prepare Fe-based MG micro-wires and the subsequent plain weaving of the glassy wires. By controlling the wire diameters, the mesh size of the wire-woven grid can be tuned. This novel Fe-B glassy microwire grid exhibits superior degradation activity and reusability when compared with commercial pure Fe powders and glassy ribbons with the same composition. The findings are expected to provide new opportunities of MGs for future applications in wastewater treatment and shed some light on designing the grid structured multicomponent metal catalysts with excellent performances.

2. Experimental

2.1. Materials

High-purity metal raw materials of Fe and B and 300 mesh Fe powders (purity >

99.5%) were purchased from Trillion Metals Co., Ltd (Beijing, China). Direct blue 15 (DB 15, $C_{34}H_{27}N_6NaO_{16}S_4$) dye was Sigma-Aldrich (America). Hydrogen peroxide (H_2O_2) solution (30%) was provided by Sinopharm Chemical Reagent Co., Ltd (Shanghai, China). All chemicals were of analytical grade and used without further purification. Deionized water (18.2 MΩ cm^{-1}) was generated by a Barnstead water system.

2.2. Preparation of $Fe_{80}B_{20}$ glassy wire woven structure.

$Fe_{80}B_{20}$ (at. %) ingot was prepared by arc-melting high purity elements (Fe: 99.99 wt.%, B: 99.9 wt.%) under a Ti-gettered argon atmosphere. The pre-alloy ingot with a weight of ~2 g was remelted in a ceramic crucible by high frequency induction heating and then the $Fe_{80}B_{20}$ glassy wire with a continuous length of over 10 meters was obtained by melt extraction using a copper wheel with a steep edge. By controlling the linear speed of the copper wheel at 30, 40 and 50 m/s, $Fe_{80}B_{20}$ glassy wires with different diameters of 97, 66 and 45 μm were produced, respectively. The $Fe_{80}B_{20}$ glassy wires were then manufactured into grid structure by plain weaving method: each $Fe_{80}B_{20}$ glassy wire was woven alternately over and under the warp glassy wires through the cloth at 90-degree angle. The mesh sizes of the $Fe_{80}B_{20}$ glassy wire grids were tuned in the range of 68 to 134 μm by using the glassy wires with different diameters.

2.3. Microstructure characterization.

Structural features of the $Fe_{80}B_{20}$ glassy microwire grids were characterized by X-ray diffraction (XRD, Rigaku DMAX-RB-12KW, Cu-Kα), scanning electron

microscopy (SEM, Zeiss Supra 55) equipped with an energy dispersive X-ray spectrometer (EDS) and transmission electron microscope (TEM, Tecnai G2 F30). A Brunauer-Emmett-Teller (BET) test was also carried out to measure the internal surface area of the samples by N_2 absorption/desorption analysis conducted at 77 K.

2.4. Azo dye degradation measurement.

The aqueous solution of DB 15 dye with the concentration of 0.2 g/L was used to evaluate the degradation performance of the samples. H_2O_2 with a concentration of 5 mM was added into the azo dye solution for oxidative degradation based on the Fenton-like reaction **[28]**. $Fe_{80}B_{20}$ glassy grids with a dosage of 0.3 g/L were used for degradation. Commercial pure Fe power (300 mesh) and $Fe_{80}B_{20}$ glassy ribbons (2~3 mm in width and 25~30 μm in thickness) with the same dosage were also tested for comparison. All experiments were conducted in 250 mL bottles, which were placed in a temperature-controlled water-bath trough. During each reaction, the solutions were rod-stirred at a constant speed. After degradation, 3 mL of filtered dye solution was pipetted out and subjected to UV-vis spectrum scanning at the wavelengths ranging from 200 to 1000 nm by using a UV spectrophotometer (UV-2800, Unico).

3. Results and discussion

Fig. 1a shows a partial configuration of the flexible wire grid specimen (20×20 mm^2) fabricated by plain weaving the melt extracted $Fe_{80}B_{20}$ wires with an average diameter of ~45 μm. It is seen that the $Fe_{80}B_{20}$ wires retain a high degree of mechanical flexibility after weaving. The high bending ability of the wires is mediated by dense

shear bands around the bending region, as shown in **Fig. 1b**. The corresponding SEM image of surface profile of the glassy wire grid is shown in **Fig. 1c**. As can be seen, the $Fe_{80}B_{20}$ grid exhibits a uniform network structure and the mesh size was estimated to be ~68 μm. The XRD pattern shown in the inset of **Fig. 1c** displays a characteristic broad halo around 45°, demonstrating the amorphous structure of the $Fe_{80}B_{20}$ wire grid. The amorphous nature of the $Fe_{80}B_{20}$ microwire is further confirmed by high resolution TEM image (**Fig. 1d**) and corresponding selected area electron diffraction (SAED) pattern (the inset in **Fig. 1d**), in which neither crystalline lattice fringes nor crystalline diffraction spots were observed. By the BET test at 77 K, the special surface area of the produced $Fe_{80}B_{20}$ glassy wire grid was measured to be 0.518 m^2/g, much higher than that of the $Fe_{80}B_{20}$ glassy ribbons (0.0236 m^2/g). Obviously, the high BET surface area is mainly benefited from the grid structure.

    Fig. 2a shows a typical UV-vis spectra of the DB 15 aqueous solution treated by the $Fe_{80}B_{20}$ glassy wire grid for different reaction periods at room temperature. It is seen that the original DB 15 solution has a strong absorption peak at around 580 nm, and the absorption peak diminishes quickly with the prolonged treatment time, indicating the continuously rapid degradation of the DB 15 dye. The solution gradually becomes light red and then fully transparent after being degraded by the $Fe_{80}B_{20}$ glassy wire grid for less than 30 min (the inset in **Fig. 2a**). These results demonstrate that the $Fe_{80}B_{20}$ glassy grid has excellent decoloration performance for the DB 15 dye aqueous solution. To further evaluate the efficiency of the glassy wire grid in degrading the DB 15 aqueous solution, comparative experiments of different catalysts including $Fe_{80}B_{20}$ glassy

ribbons and pure Fe powders with the same dosage for degradation were carried out at room temperature. By measuring the intensity of the DB adsorption peak at ~580 nm, the normalized concentration (C_t/C_o, where C_t is the measured intensity for different reaction times and C_o is the original intensity) variations of the DB 15 aqueous solution as a function of degradation time for the catalysts studied are presented in **Fig. 2b**. It is seen that the normalized concentration decreases insignificantly without catalyst, suggesting that the added 5mM H_2O_2 cannot decompose the DB 15 dye alone at room temperature. For pure Fe powders in this given dosage, the decoloration of the DB 15 aqueous solution is still very slow (more than 120 min), but the $Fe_{80}B_{20}$ glassy ribbon catalysts degraded the dye solution in a short time. This improvement is due to the metastable state of the Fe-based MGs, which enables the superficial Fe active atoms keep high reaction activity during degradation **[27]**. For all samples, the decomposition behaviors can be well fitted by the pseudo-first-order kinetic model **[25, 29]**:

$$C_t/C_o = C_1 + C_2\exp(-t/t_0)$$

where C_t/C_o is the normalized concentration of DB 15, C_1 and C_2 are fitting constants, t is the reaction time and t_0 is the time when the concentration decreases to e^{-1} of the initial condition. The degradation efficiency can be simply evaluated by the value of t_0. In this case, the calculated results show that the current $Fe_{80}B_{20}$ glassy wire grid exhibits superior efficiency (~ 4.3 min), 2.1 times faster than that of the $Fe_{80}B_{20}$ glassy ribbons and 28 times for pure Fe powders in degrading the DB 15 dye. This value is also much higher than that of the reported Fe-based metallic glass powder (16 min) **[25]**, glassy FeSiB ribbon (8.7 min) **[30]**, ball-milled AlCrFeCoNi and

FeCoNiCrMn high entropy alloy powders (8.4-9.6 min) [31], manifesting its great potential to be utilized as high efficiency catalyst material for purifying dyeing wastewater.

To understand the enhancement effect of the wire grid structure for the decomposition of DB 15 dye, the difference in reaction kinetics between the $Fe_{80}B_{20}$ glassy grids and ribbons was investigated by measuring the normalized concentration dependence on reaction temperature. **Fig. 3a** and **3b** show the normalized concentration *vs* degradation time at different temperatures (from 25 to 55 °C) for the $Fe_{80}B_{20}$ glassy grids and ribbons, respectively. For both glassy catalysts, the degradation accelerates significantly as the reaction temperature increases, demonstrating that the degradation is a thermally activated reaction process. Based on the t_0 value at different temperatures obtained by data fitting, the thermal activation energy can be then estimated according to the Arrhenius-type equation [30, 32]:

$$\ln t_0 = E_a/RT + \ln A$$

where E_a is the activation energy, R is the gas constant, T is the reaction temperature and A is a constant. The Arrhenius plots of $\ln k_T$ versus $1000/RT$ for the $Fe_{80}B_{20}$ glassy grids and ribbons are further shown in the inset of **Fig. 3a** and **3b**, respectively. The calculated E_a for the glassy grid is approximately 37.4 kJ/mol, lower than that of the glassy ribbon, i.e.,49.1 kJ/mol. The smaller activation energy of the grids indicates that the decoloration reaction is easier to proceed, which is resulted from the higher internal surface area, providing more effective contact area and more active sites for the azo dye, thereby leading to a significant improvement of the degradation

efficiency. The influence of the glassy grid structure on the degradation efficiency was then investigated. The insets in **Fig. 3c** exhibit the surface morphologies of grid structures with different wire diameters and mesh sizes, and their surface areas are 0.518 (a), 0.373 (b) and 0.265 m^2/g (c), respectively. As shown in **Fig. 3c**, the degradation of the DB dye is significantly accelerated as the pore size and wire diameter of the grid structure decrease, further manifesting that the increased internal surface area of the grids contributes to the high degradation efficiency. It is also known that solution PH is another important factor in iron-contaminant systems for wastewater treatment. Thus we further investigate the relationship between solution PH and degradation performance of the $Fe_{80}B_{20}$ glassy wire grid structure. **Fig. 3d** shows the effect of initial solution PH ranging from 3 to 10 on the degradation of 0.2 g/L DB 15 solution by 0.3 g/L grid sample with mesh size of ~68 μm. It is seen that the degradation rate of DB 15 decrease with the increase of PH. High degradation ratio is maintained for pH≤7. As the pH increases up to 10, the degradation ratio of DB 15 decrease to ~90% at 60 min. This is because that the surface of $Fe_{80}B_{20}$ glassy wire grid can be positively charged at lower PH, which is benefit for the adsorption of DB 15 dye molecules with sulfonic groups onto the iron surface **[30]**. When the solution pH is above the isoelectric point, the negatively charged surface could be easily covered by corrosion products which will decrease the number of active sites and inhibit the electron transfer, thus result in a low degradation efficiency. The result also indicates that for practical application, there is no need to add more acid solution into the reaction system to ensure acid environment for complete degradation.

The structural stability and reusability of the glassy grids have also been evaluated by cyclic degradation. **Fig. 4a** demonstrates the surface morphology of the $Fe_{80}B_{20}$ glassy grids after the decomposition process, which reveals that the grid structure kept porous and the reaction products distribute uniformly on the $Fe_{80}B_{20}$ glassy wire ligaments. Meanwhile, the XRD spectrum in the inset shows that the $Fe_{80}B_{20}$ wire grid remains amorphous after degradation. This observation indicates that the DB 15 molecules only react with the surface active atoms of the $Fe_{80}B_{20}$ MGs during degradation and the base glassy structure is still stable. The EDS results for the surface of the initial $Fe_{80}B_{20}$ glassy wire grid sample and the sample reacted with DB 15 azo dye solution are shown in **Fig. 4b** and **c**, respectively (The relative changes in the composition of the component elements are accordingly presented in the insets). It is seen that after the degradation process, no obvious changes of the composition are detected. This denotes that the glassy $Fe_{80}B_{20}$ react uniformly with azo dye without compositional alteration. **Fig. 4d** further shows the cycling life of the grid structure during degradation, confirming that the degradation ratio (at 30 min) still remains ∼94 % after 5 cycles without obvious activity loss. While for commercial Fe powders in practical application, due to the high corrosion rate of crystalline Fe powders, the degradation ratio declines sharply (65% at 120 min) after the first use **[17, 33]**, this comparison further indicates the reusability of the $Fe_{80}B_{20}$ wire grid structure in industry application. Moreover, it should be noted that, unlike particulate catalyst, the glassy wire grid can be easily separated from the dye solution without any centrifuge operation after degradation and reused again. This is because of the monolithic structure of the

grid sample, which can effectively prevent the dispersion of the catalyst in dye solution during degradation. Meanwhile, in practical applications, this glassy grid structure with micro-scale mesh size ranging from 68 to 134 μm can be also served as filter net to remove impurities with particle size of over 70 μm, such as fiber tows or other suspended solids in printing and dyeing wastewater during degradation. These advantages further endow these glassy wire grids great potential for applications in sewage purification. The next step for this work is to improve the grid structure with higher surface area by using thinner glassy wires or dealloying for surface nanoporous structure, for the purpose of further boosting the degradation efficiency.

4. Conclusions

In summary, flexible $Fe_{80}B_{20}$ glassy wire grid structures with tunable mesh size are newly designed and can be easily fabricated by melting spinning and subsequent plain weaving. The glassy wire grids exhibit superior reaction efficiency and reusability in degrading the DB 15 dye solution, as compared with commercial pure Fe powders and $Fe_{80}B_{20}$ glassy ribbons. The excellent degradation performance is attributed to the uniform grid structure with high internal surface area. Our findings manifest that the newly designed glassy $Fe_{80}B_{20}$ wire grids have great potential to be utilized as high-efficiency catalyst for purifying wastewater in industry. Also the current study broadens the application ranges of metallic glasses and enlightens the design of high-performance grid structured multicomponent metal catalysts.

Acknowledgements

Conflict of interest

The authors declare that they have no conflict of interest.

References

[1] G. Mishra, M. Tripathy, A critical review of the treatment for decolorization of textile effluent, Colourage 40(10) (1993) 35-38.

[2] V.K. Gupta, Suhas, Application of low-cost adsorbents for dye removal--a review, J. Environ. Manage. 90(8) (2009) 2313.

[3] T. Robinson, G. Mcmullan, R. Marchant, P. Nigam, Remediation of dyes in textile effluent: a critical review on current treatment technologies with a proposed alternative, Bioresour. Technol. 77(3) (2001) 247-55.

[4] C.Y.P. Ayekoe, D. Robert, D.G. Lanciné, Combination of coagulation-flocculation and heterogeneous photocatalysis for improving the removal of humic substances in real treated water from Agbô River (Ivory-Coast), Catal. Today 281 (2017) 2-13.

[5] K. Im, D.N. Nguyen, S. Kim, H.J. Kong, Y. Kim, C.S. Park, O.S. Kwon, H. Yoon, Graphene-embedded hydrogel nanofibers for detection and removal of aqueous-phase dyes, ACS Appl. Mater. Inter. 9(12) (2017) 10768-10776.

[6] K.R. Reddy, M. Hassan, V.G. Gomes, Hybrid nanostructures based on titanium dioxide for enhanced photocatalysis, Appl. Catal. A: Gen. 489 (2015) 1-16.

[7] C. Cara, E. Rombi, A. Musinu, V. Mameli, A. Ardu, M.S. Angotzi, L. Atzori, D. Niznansky, H. Xin, C. Cannas, MCM-41 support for ultrasmall γ-Fe$_2$O$_3$ nanoparticles for H$_2$ S removal, J. Mater. Chem. A 5(41) (2017) 21688-21698.

[8] K.R. Reddy, V.G. Gomes, M. Hassan, Carbon functionalized TiO$_2$ nanofibers for high efficiency photocatalysis, Mater. Res. Express 1(1) (2014) 015012.

[9] K.R. Reddy, K. Nakata, T. Ochiai, T. Murakami, D.A. Tryk, A. Fujishima, Facile

fabrication and photocatalytic application of Ag nanoparticles-TiO$_2$ nanofiber composites, J. Nanosci. Nanotechno. 11(4) (2011) 3692-3695.

[10] K.R. Reddy, K. Karthik, S.B. Prasad, S.K. Soni, H.M. Jeong, A.V. Raghu, Enhanced photocatalytic activity of nanostructured titanium dioxide/polyaniline hybrid photocatalysts, Polyhedron 120 (2016) 169-174.

[11] J. Cao, L. Wei, Q. Huang, L. Wang, S. Han, Reducing degradation of azo dye by zero-valent iron in aqueous solution, Chemosphere 38(3) (1999) 565.

[12] S. Nam, P.G. Tratnyek, Reduction of azo dyes with zero-valent iron, Water Res. 34(6) (2000) 1837-1845.

[13] H. Li, J. Guo, L. Yang, Y. Lan, Degradation of methyl orange by sodium persulfate activated with zero-valent zinc, Sep. Purif. Technol. 132 (2014) 168-173.

[14] J. Fan, Y. Guo, J. Wang, M. Fan, Rapid decolorization of azo dye methyl orange in aqueous solution by nanoscale zerovalent iron particles, J. Hazard. Mater. 166(2) (2009) 904-910.

[15] L.G. Devi, S.G. Kumar, K.M. Reddy, C. Munikrishnappa, Photo degradation of Methyl Orange an azo dye by Advanced Fenton Process using zero valent metallic iron: Influence of various reaction parameters and its degradation mechanism, J. Hazard. Mater. 164(2) (2009) 459-467.

[16] M. Kallel, C. Belaid, R. Boussahel, M. Ksibi, A. Montiel, B. Elleuch, Olive mill wastewater degradation by Fenton oxidation with zero-valent iron and hydrogen peroxide, J. Hazard. Mater. 163(2) (2009) 550-554.

[17] M. Velimirovic, P.O. Larsson, Q. Simons, L. Bastiaens, Effect of boron on

reactivity and apparent corrosion rate of microscale zerovalent irons, J. Environ. Chem. Eng. 5(2) (2017) 1892-1898.

[18] F.L. Fu, D.D. Dionysiou, H Liu, The use of zero-valent iron for groundwater remediation and wastewater treatment: a review, J. Hazard. Mater. 267 (2014) 194-205.

[19] A.L. Greer, Metallic glasses, Science 2(4) (1997) 1947-1953.

[20] Á. Molnáar, G.V. Smith, M. Bartók, New catalytic materials from amorphous metal alloys, Adv. Catal. 36(6) (1989) 329-383.

[21] Y.C. Hu, Y.Z. Wang, R. Su, C.R. Cao, F. Li, C.W. Sun, Y. Yang, P.F. Guan, D.W. Ding, Z.L. Wang, A highly efficient and self-stabilizing metallic-glass catalyst for electrochemical hydrogen generation, Adv. Mater. 28(46) (2016) 10293.

[22] Z. Jia, W. Zhang, W. Wang, D. Habibi, L. Zhang, Amorphous $Fe_{78}Si_9B_{13}$ alloy: An efficient and reusable photo-enhanced Fenton-like catalyst in degradation of cibacron brilliant red 3B-A dye under UV-vis light, Appl. Catal. B: Environ. 192 (2016) 46-56.

[23] J.Q. Wang, Y.H. Liu, M.W. Chen, G.Q. Xie, D.V. Louzguine−Luzgin, A. Inoue, J.H. Perepezko, Rapid degradation of azo dye by Fe-based metallic glass powder, Adv. Funct. Mater. 22(12) (2012) 2567-2570.

[24] C. Zhang, H. Zhang, M. Lv, Z. Hu, Decolorization of azo dye solution by Fe-Mo-Si-B amorphous alloy, J. Non-Cryst. Solids 356(33–34) (2010) 1703-1706.

[25] J.Q. Wang, Y.H. Liu, M.W. Chen, D.V. Louzguine-Luzgin, A. Inoue, J.H. Perepezko, Excellent capability in degrading azo dyes by MgZn-based metallic glass powders, Sci. Rep. 2(5) (2012) 418.

[26] Y.F. Zhao, J.J. Si, J.G. Song, Q. Yang, X.D. Hui, Synthesis of Mg-Zn-Ca metallic

glasses by gas-atomization and their excellent capability in degrading azo dyes, Mater. Sci. Eng. B 181(181) (2014) 46-55.

[27] X.D. Qin, Z.W. Zhu, G. Liu, H.M. Fu, H.W. Zhang, A.M. Wang, H. Li, H.F. Zhang, Ultrafast degradation of azo dyes catalyzed by cobalt-based metallic glass, Sci. Rep. 5 (2015) 18226.

[28] Z. Deng, X. Zhang, K. Chan, L. Liu, T. Li, Fe-based metallic glass catalyst with nanoporous surface for azo dye degradation, Chemosphere 174 (2017) 76-81.

[29] H.-Y. Shu, M.-C. Chang, H.-H. Yu, W.-H. Chen, Reduction of an azo dye Acid Black 24 solution using synthesized nanoscale zerovalent iron particles, J. Colloid Interf. Sci.314(1) (2007) 89-97.

[30] Y. Tang, Y. Shao, N. Chen, X. Liu, S. Chen, K. Yao, Insight into the high reactivity of commercial Fe-Si-B amorphous zero-valent iron in degrading azo dye solutions, Rsc Adv. 5(43) (2015) 34032-34039.

[31] Z. Lv, X. Liu, B. Jia, H. Wang, Y. Wu, Z. Lu, Development of a novel high-entropy alloy with eminent efficiency of degrading azo dye solutions, Sci. Rep. 6 (2016) 34213.

[32] R. Li, K.C. Chan, X.J. Liu, X.H. Zhang, L. Liu, T. Li, Z.P. Lu, Synthesis of well-aligned CuO nanowire array integrated with nanoporous CuO network for oxidative degradation of methylene blue, Corros. Sci. 126 (2017) 37-43.

[33] C.-H. Weng, Y.-T. Lin, C.-K. Chang, N. Liu, Decolourization of direct blue 15 by Fenton/ultrasonic process using a zero-valent iron aggregate catalyst, Ultrason. Sonochem. 20(3) (2013) 970-977.

Figure Captions

Fig. 1. (a) Configuration of glassy wire grids fabricated by weaving $Fe_{80}B_{20}$ MG wires. (b) SEM image of a flexible $Fe_{80}B_{20}$ MG wire. (c) Surface morphology of the $Fe_{80}B_{20}$ MG grid, and the inset is the XRD spectra of the microwire grid. (d) TEM image of the $Fe_{80}B_{20}$ microwire, and the inset shows the corresponding SAED pattern.

Fig. 2. (a) UV absorption spectrums of 20.2 g/L DB 15 aqueous solution degraded by $Fe_{80}B_{20}$ glassy wire grids for different reaction times at room temperature. The inset shows the appearance and color change of the DB 15 solution during degradation. (b) The normalized concentration of DB 15 solution at 580 nm versus the reaction time for different samples at room temperature.

Fig. 3. The normalized concentration of DB 15 solution at ~580 nm as a function of reaction time at different temperatures for $Fe_{80}B_{20}$ glassy wire grids (a) and ribbons (b) with the same dosage. The inset in (a) and (b) is the Arrhenius plot of $\ln k_T$ versus $1000/RT$ of DB 15 degradation by the wire grids and ribbons, respectively. (c) The normalized concentration of DB 15 solution at ~580 nm versus the reaction time for $Fe_{80}B_{20}$ glassy wire grids with different mesh sizes. The insets show the SEM images of the grid structures with different mesh sizes. (d) Effect of solution PH on the degradation of 200 mg/L DB 15 solution by 0.3 g/L $Fe_{80}B_{20}$ glassy wire grid.

Fig. 4. (a) Surface morphology and XRD spectrum (inset) of the $Fe_{80}B_{20}$ glassy wire grid after the degradation process. (b) EDS analysis of the initial $Fe_{80}B_{20}$ glassy wire grid sample. (c) EDS analysis of the sample reacted with DB 15 azo dye solution. (d) Cyclic degradation test of the $Fe_{80}B_{20}$ glassy wire grid on the 0.2 g/L DB 15 aqueous solution.
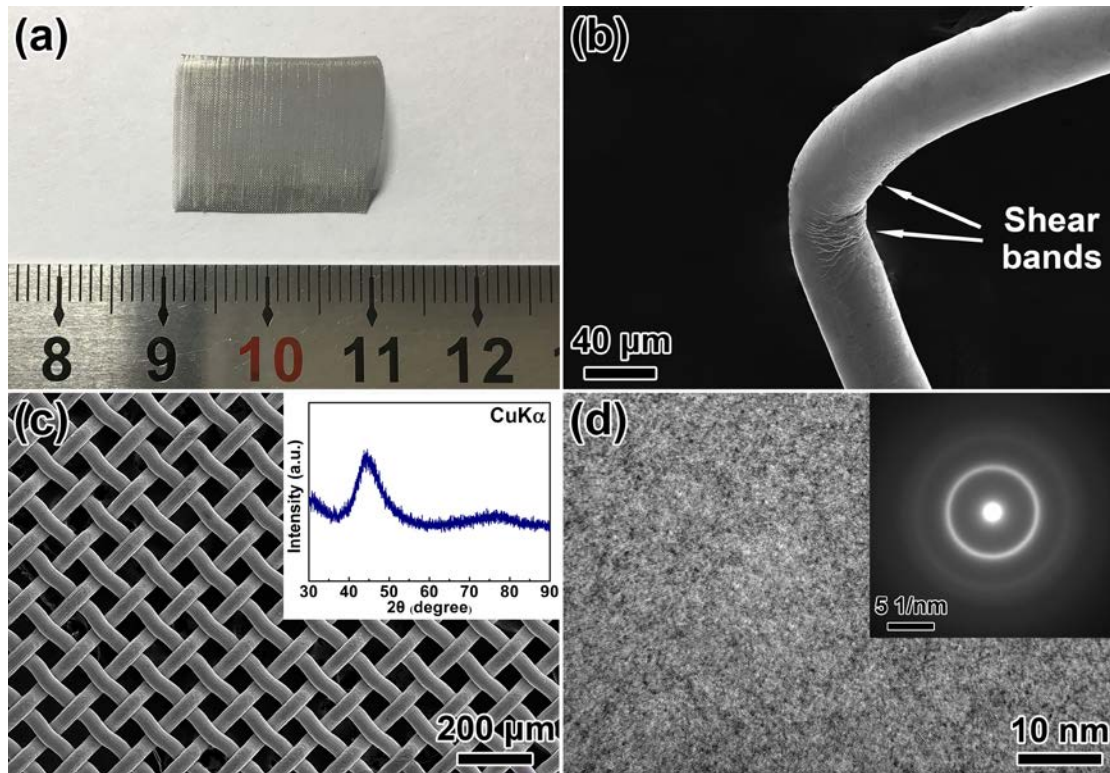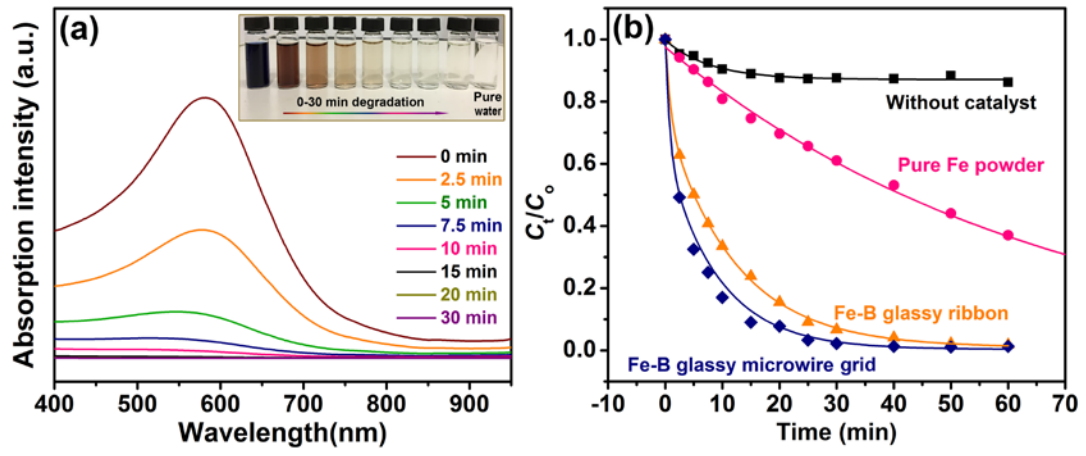
Fig. 1 by Li et al.
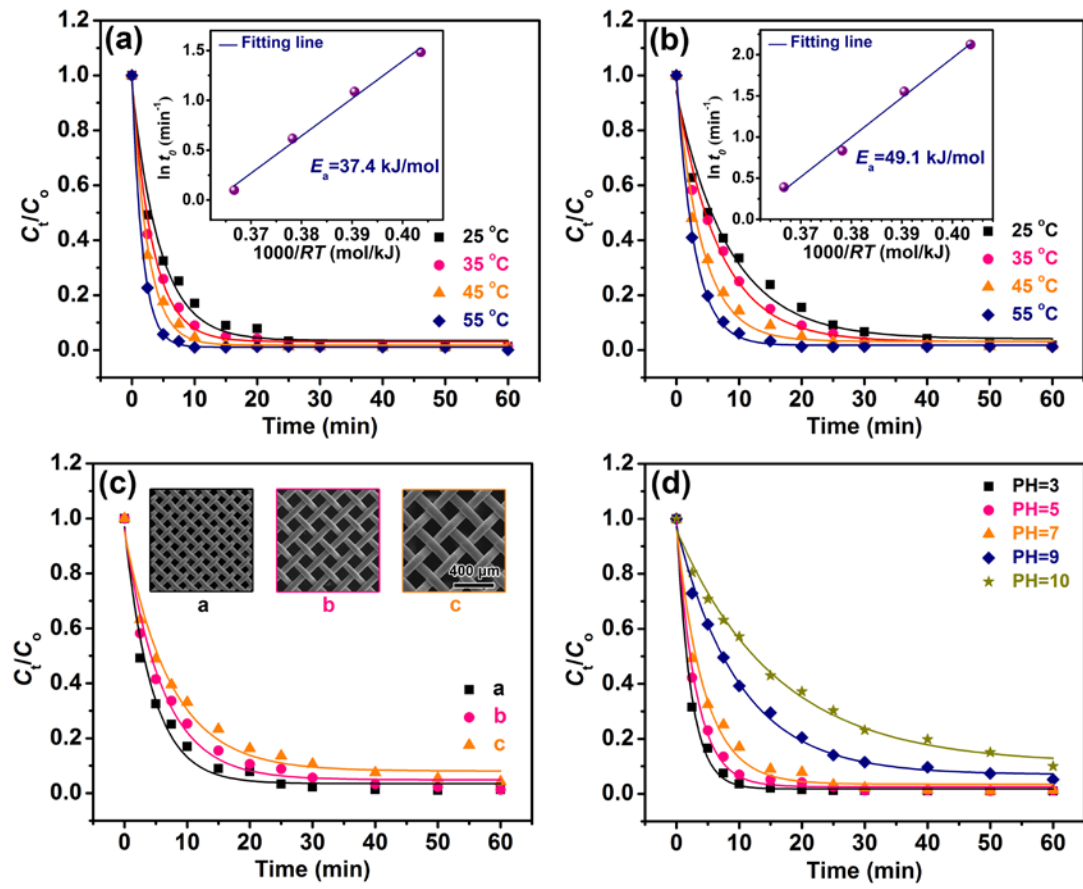
Fig. 2 by Li et al.

Fig. 3 by Li et al.

Fig. 4 by Li et al.